Metallography, Microstructure, and Analysis (2022) 11:704–710
https://doi.org/10.1007/s13632-022-00889-0

PEER-REVIEWED PAPER

Exploring the Strengthening Effect of Carbide Precipitation in Fe-18Mn-2Cr-1C-4Al(wt.%) Lightweight Steel

Zhibin Zheng[1] · Haokun Yang[2] · A. P. Shatrava[3] · Yi Yang[1] · Jun Long[1] · Kaihong Zheng[1,4]

Received: 20 May 2022 / Revised: 6 September 2022 / Accepted: 6 September 2022 / Published online: 16 September 2022

Abstract

The Fe-18.4Mn-2.1Cr-1.3C-4Al (wt.%) steel was designed for lightweight application purpose with comprehensive advantages of low density, wear resistance, and high strength. Further exploring of the mechanical properties, especially the yield strength influenced by the aging treatments (300 °C and 500 °C), needs more investigation. The precipitated carbides observations and tensile tests, after specific solution and aging treatments, were carried out to reveal that the $Fe(Mn)_3C$ carbide precipitation contributed up to 111 MPa strengthening effect on yield strength with 300 °C aging heat treatment. The present study pointed out that tailor-made solution and aging treatments processes to achieving further strength improvement, especially for yield stress.

Keywords Lightweight steel · Yield strength · Aluminum · $Fe(Mn)_3C$ carbide · Precipitation

Introduction

Developing high strength and low-density high manganese steel is one of the opportunities and also the challenges for energy-efficient and eco-friendly requirements [1]. The previous study revealed that the addition of Al element into high manganese steel brought considerable density reduction of 1.5% weight reduction with 1 wt.% Al [2]. To pursue higher strength and ductility of high manganese steel, the utilization of fully austenitic matrix with nanoparticle precipitation [3–5], duplex phase of ferrite/austenite [6, 7], twinning/transformation-induced plasticity (TWIP/TRIP) mechanisms [8], as well as grain refinement by severe plastic deformation [9] were considered and made positive progress.

As the request of high strength for structural steel products becomes stricter, the upgraded steel must possess yield stress of more than 460 MPa [10] to meet the target. According to the above strengthening mechanisms, only secondly phase precipitation and grain refinement processes have significant improvement on yield strength. However, the previous study proved that the grain refinement method sacrificed the ductility, resulting in unqualified industry and safety requirements [11]. Luckily, the carbide precipitation-strengthening mechanism improves the yield strength obviously, while possessing limited loss of the plastic ductility [12]. Lu et al. [13] applied Thermo-Calc software to predict the equilibrium concentration of C, Al, and Mn elements dissolving in the austenitic matrix. The result showed that the high Al partitioning and fast diffusion of C obviously contribute to carbides nucleation with aging temperature. With the completion of the Al–Fe and Al–Mn binaries, Lindahl and Selleby improved the Fe–Mn–Al system to provide a reliable assessment of the carbides precipitation with temperature [14].

It thus appears that suitable heat treatment on the Fe–Mn–Al lightweight steel shall facilitate the incubation of fine carbide in the metallic matrix, providing an effective way to improve yield strength while preserving plastic

Zhibin Zheng and Haokun Yang have contributed equally.

✉ Haokun Yang
hkyang@hkpc.org

1 Institute of New Materials, Guangdong Provincial Key Laboratory of Metal Toughening Technology and Application, Guangdong Academy of Sciences, Guangzhou 510650, People's Republic of China

2 Smart Manufacturing Division, Hong Kong Productivity Council, Hong Kong SAR 999077, Hong Kong, People's Republic of China

3 Physicotechnological Institute of Metals and Alloys, National Academy of Sciences, Kiev, Ukraine

4 Guangdong Provincial Iron Matrix Composite Engineering Research Center, Guangzhou 510650, People's Republic of China

ductility for lightweight steel design and application. In the previous study, Ishida et al. [15] figured out that the $Fe(Mn)_3AlC$ carbide was commonly observed in high manganese and low Al content (< 8 wt.%) or without Al content steel after heat treatment [16]. Hwang et al. [3] reported that the presence of fine carbides within austenite grains and along the grain boundary provided an additional strengthening effect on the ultrahigh yield stress. Shun et al. [17] pointed out that the M_3C carbide induced additional strain hardening by the solute-dislocation pinning process. Moreover, the precipitation-strengthening mechanism under aging treatment also works in Al–Mn–Cr–Zr alloys [18]. However, the quantitative study of the precipitation-strengthening mechanism in high manganese steel, especially the effect of solution and aging treatments on the strengthening mechanism, was seldom reported.

Materials and Methods

The chemical composition of studied steel is Fe-18.4Mn-2.1Cr-1.3C-4Al (wt.%, short for ZG4Al), and the 30 KG ingot was melted in vacuum medium frequency induction melting furnace. The solution treatment was carried out under temperature of 1100 °C for 3 h following furnace cooling, and aging treatment between 300 and 500 °C for 4 h, following with water quenching.

The ZG4Al steel samples were polished and etched in aquaregia, and then the microstructure of ZG4Al sample was observed under Leica DMI 3000 M optical microscope (OM) and Quanta200 scanning electron microscope (SEM). The grain size of the treated ZG4Al steel is measured by the line intercept method.

The TEM thin foils were spark cut from the undeformed samples, mechanical polished, and thinned under Gatan 695 ion thinning equipment. The microstructure was observed under FEI Talos F200X transmission electron microscope (TEM). The element composition of the precipitation was measured by energy dispersive x-ray Spectroscopy (EDS) under SEM and TEM.

After heating treatment, a gage length and diameter of 20 and 5 mm tensile samples were prepared by machining. All the samples were mechanical polished to 2000# SiC paper to remove the deformed layer. Tensile tests were performed using WDW-150E universal testing machine equipped with an extensometer at room temperature, and the tensile strain rate is 1.6×10^{-3} s^{-1}.

Results and Discussion

To directly observe the evolution of carbide precipitation influenced by solution and aging treatments, the OM observation method is chosen. Figure 1 illustrates the microstructure of the ZG4Al sample with 1100 °C solution and different aging treatments from 300 to 500 °C. The present observation reveals that the ZG4Al steel is fully austenitic structure. The grain sizes of the 1100 °C solution treated,

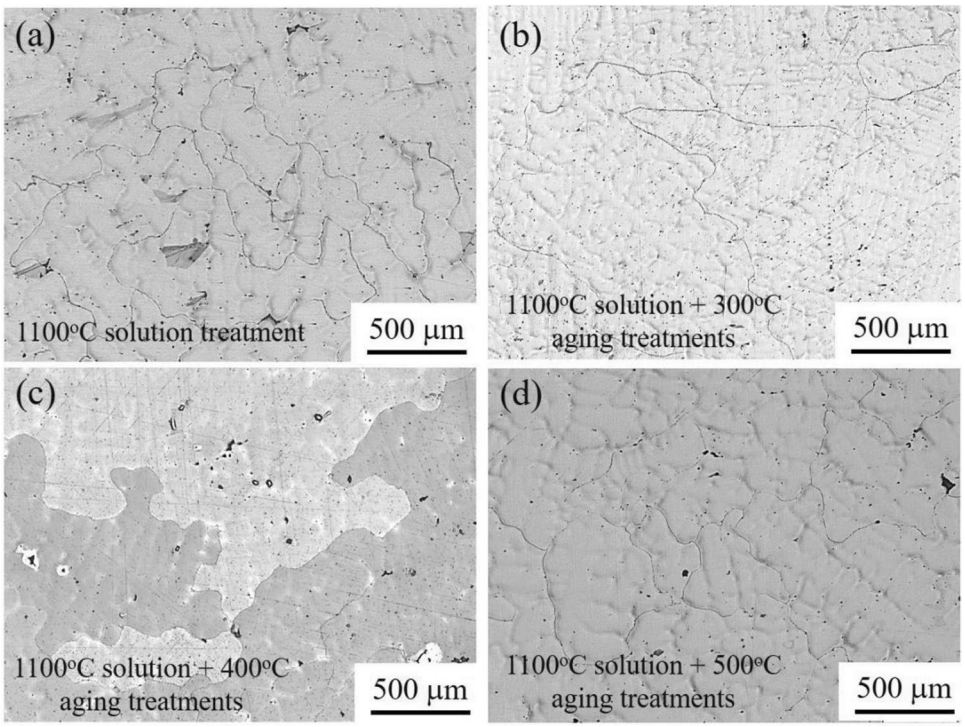

Fig. 1 Microstructure observation of ZG4Al steel with different solution and aging treatments: (**a**) 1100 °C solution treatment, (**b**) 1100 °C solution + 300 °C aging treatments, (**c**) 1100 °C solution + 400 °C aging treatment, and (**d**) 1100 °C solution + 500 °C aging treatment

solution and 300 °C aging treated, solution and 400 °C aging treated, solution and 500 °C aging treated samples are measured to be 487, 588, 588, and 487 μm. With observation of the precipitation, Fig. 2a reveals that the nucleation of the precipitation mostly locate within the grain, as well as along the grain boundary directly after solution treatment. The magnification of the OM observation is chosen to be 200X for better calculation and comparison of the size and distribution of the precipitates. With an additional 300 °C aging treatment, the distribution density and the location of the precipitation do not change much as shown in Fig. 2b. However, with 400 °C aging treatment, the precipitations dissolved both at the grain boundary and inside the grain (Fig. 2c). During the 500 °C aging treatment, the precipitations are hardly observed within grain, meanwhile some of the precipitations dissolved along the grain boundary as shown in Fig. 2d.

To make a clear comparison of the size and distribution density of the precipitations, the statistical result of the precipitation size is measured to be 4.76 ± 2.12, 4.64 ± 2.03, 5.53 ± 2.17, and 5.51 ± 2.66 μm with aging temperature increasing, respectively. It means that the subsequently aging treatment has little effect on the precipitation size. It shall be noted that the precipitations with nanoscale are hardly observed under SEM, but the above comparison data can provide the reference to study the effect of aging treatment on precipitating. In the meanwhile, the density of precipitation is getting higher with 300 °C aging treatment from 211 to 278 particles/mm^2. With further aging temperature increasing, the precipitation density decreases to 117 particles/mm^2 (400 °C aging treatment) and 92 particles/mm^2 (500 °C aging treatment). Nurjaman et al. [19] reported that the high Mn steel with 400 °C aging treatment, after 950 °C solution treatment, exhibits optimum hardness and fine carbides dispersion within the matrix. However, after higher aging temperature treatments, the lower hardness was measured, and the carbides dissolved.

The above observation result supports that the precipitation formation has strong connection with the solution and aging treatment. Therefore, with the controlling of heating treatment, the effect of precipitation on the mechanical properties, especially on the yield strength, can be compared and discussed.

To measure and compare the chemical composition of the precipitation, the particle with a scale between 50 and 100 nm is chosen for reliable chemical composite detection by SEM equipped with EDS as shown in Fig. 3a and b. The result shows that the precipitation in 300 °C aging treated ZG4Al steel has a much higher content of C and Mn elements, while the content of Cr, Al, and Fe elements drastically decreases compared with that of the matrix. The repeated detections of the precipitation composition are close and consistent, showing that the precipitation is M_3C carbide, which is also reported in [20]. Furthermore, the composition of the precipitation is also examined under TEM (in Fig. 3c), where the precipitation has 60.29 at.% of C element. This observation result is also consistent with the EDS result under SEM. It shall be noted

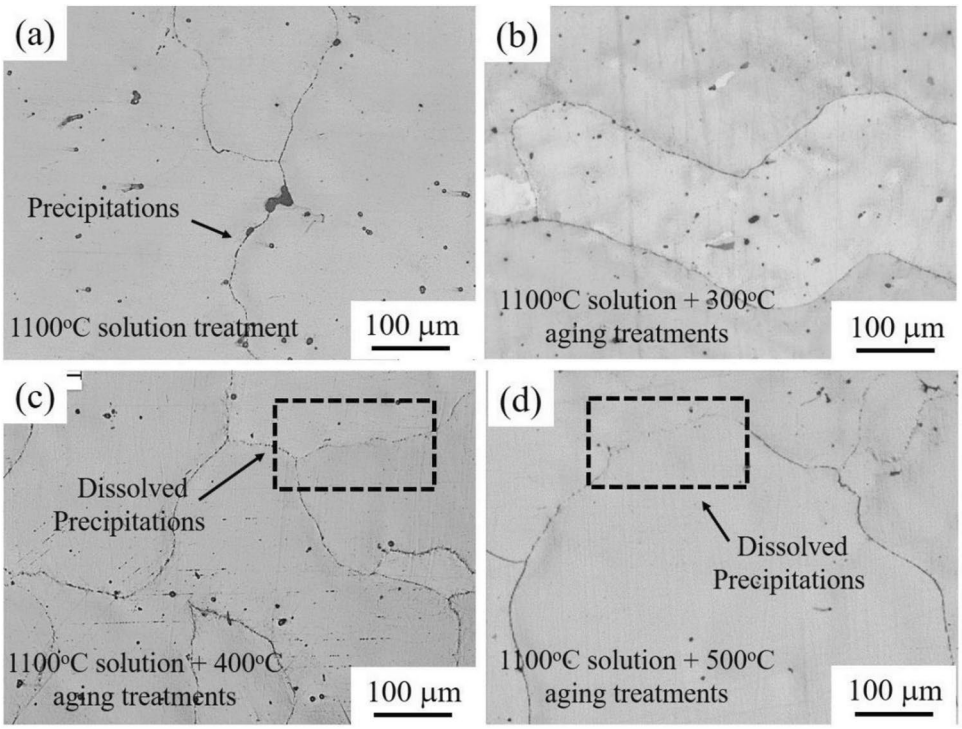

Fig. 2 Detailed observation of the precipitation in ZG4Al steel with different solution and aging treatments: (**a**) 1100 °C solution treatment, (**b**) 1100 °C solution + 300 °C aging treatments, (**c**) 1100 °C solution + 400 °C aging treatment, and (**d**) 1100 °C solution + 500 °C aging treatment

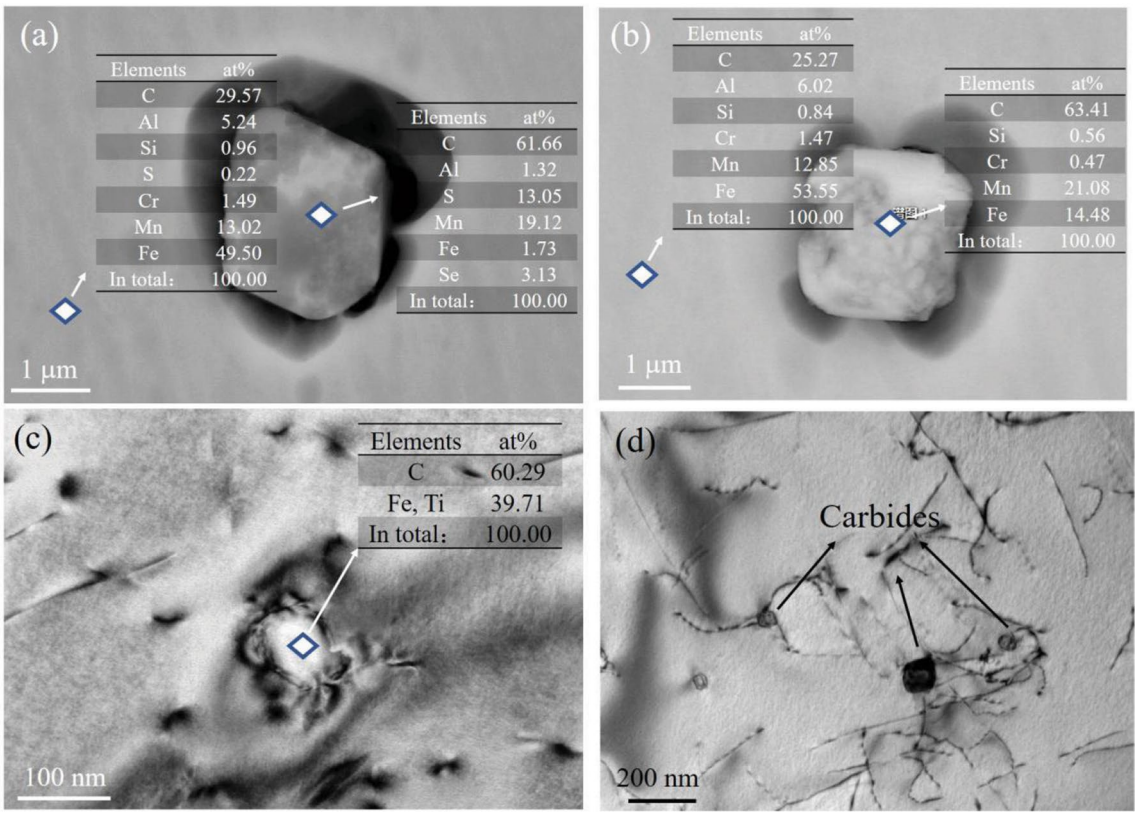

Fig. 3 (**a** & **b**) Morphology and composition of the precipitations under SEM, and (**c** & **d**) precipitation composition and interaction between precipitation and dislocations under TEM observation in 300 °C aging treated ZG4Al steel, respectively

Table 1 Tensile properties of ZG4Al steel after solution and aging treatments

Solution temperature, °C	Aging temperature, °C	Yield stress, σ_y, MPa	Ultimate tensile strength, σ_b, MPa	Uniform elongation, %	Strain hardening coefficient, σ_b/σ_y
1100	Nil	450	713	51.4	1.58
1100	300	456	754	34.5	1.65
1100	400	430	695	38.5	1.62
1100	500	392	683	33.5	1.74

that the size of observed precipitation under SEM is close to micron level, while other nanoscale carbides are not counted.

Besides, the strip pattern is found around the $Fe(Mn)_3C$ carbide, illustrating microstructure distortion is activated during the precipitation process, and then introduces internal stress between the matrix and carbides, as shown in Fig. 3c. What's more, the dislocations are also observed and pinned by the carbides as shown in Fig. 3d. These dislocations shall be enabled by the sample preparation and/or quenching processes, and then pinned by carbides. It thus appears that the $Fe(Mn)_3C$ carbide shall make considerable contribution to yield strength by two direct arguments: (1) Carbide precipitation process results in microstructure distortion and brings internal strengthening effect. (2) The pinned dislocation by nanoscale carbides makes further contribution to mechanical strength, especially for yield stress.

The mechanical properties of the ZG4Al steel after solution and aging treatment are displayed in Table 1, where the yield stress (σ_y) slightly increases with 300 °C aging temperature and then decreases with increasing aging temperature till 500 °C. In the meanwhile, with the aging treatment temperature increasing, the ultimate tensile strength and uniform elongation of the ZG4Al steel drop. According to the present testing results, the relation between precipitations and yield stress will be discussed, as well as the contributions of grain boundary and solute elements to yield stress are also counted. In consideration of the strain hardening coefficient, uniform elongation and ultimate tensile strength are influenced by the interaction between dislocations and

deformation bands. The plastic deformation mechanism will be discussed in the other Refs. [21, 22].

Grain Boundary Strengthening

According to the Hall–Petch theory, the yield strength (σ_y) of fully recovered and single phase metallic materials have the below relation with average grain size: $\sigma_y = \sigma_0 + kd^{-1/2}$, where σ_y is the yield strength, σ_0 is the friction stress, and the k and d are the strength coefficient and average grain size. In consideration that the strength coefficient is different between Fe–Mn–C and Fe–Mn–Si–Al two series high manganese steel [23]. The strength coefficient $k = 472\ MPa\sqrt{\mu m}$ and $\sigma_0 = 133$ MPa are adopted as reference of Fe-22Mn-0.6C (wt.%) steel, which has the common element composition as the present material has. The strength contribution of grain boundary to yield stress is illustrated in Table 2. It shows that grain boundary has little difference because: (1) ZG4Al steel has coarse grain around 500 μm, (2) the aging temperature is too low for grain growth.

Solutes Strengthening

Except the grain boundary strengthening mechanism, the solutes also make contribution to the yield stress. In the present study, the solute atoms, including Mn, Al, Cr, and C are calculated based on the linear relation between chemical content and yield strength. Ding et al. [24] reported that the Mn addition into the Fe-xMn-0.6C ($18 \le x \le 30$) high manganese steel has little influence on the yield strength. This is because that Mn mainly works on the strength and hardening behavior in the later stage of plastic deformation, rather than yield strength. Thus, the strengthening effect of Mn element on yield stress is excluded here.

The mechanical properties of Fe-26Mn-0.3C-3Al-xCr ($x = 1.1$, 2.4, and 4.0) high manganese austenitic steels were also chosen [25]. The relation between Cr element content and yield strength is calculated and illustrated as: $\sigma_y = 19.69Cr_{wt.\%} + 405.4$, where the correlation index is 0.996. It thus appears that 1 wt.% addition of Cr element, the yield stress of high manganese steel increases 19.69 MPa within the range of 1–4 wt.% Cr content.

Table 2 Evaluation of strengthening contribution on yield stress of ZG4Al steel under different temperatures

Solution temperature, °C	Aging temperature, °C	Grain boundary, MPa	Solutes, MPa	Carbides, MPa
1100	Nil	154	193	103
1100	300	152	193	111
1100	400	152	193	85
1100	500	154	193	45

In the previous study, Yang et al. [26] systemically studied the effect of Al addition on high manganese steel yield stress. The results show that the yield stress of Fe-22Mn-0.6C-xAl ($x = 0$, 3, 6) steel also has linear relation with the Al element content as: $\sigma_y = 10.5Al_{wt.\%} + 351.5$ with correlation index of 0.942. As the twinning starting strain of this Fe-22Mn-0.6C steel is higher than 2% [27], which is much far away from the yield strain of the 0.2%, what is more, the Al addition suppress the twinning mechanism [26]. Therefore, the above linear equation can effectively predict the contribution of Al element to yield stress of high manganese steel with Al composition from 0 to 6 wt.%.

Carbon is the interstitial sold solution element into the high manganese steel, where the strengthen effect on yield stress shall be stronger. In the previous study, the C element addition into the Fe-30Mn-xC ($x = 0$, 0.3, 0.9) has linear increasement of yield stress as [28]: $\sigma_y = 180.71C_{wt.\%} + 205.71$ with 0.999 correlation index, indicating the composition of C has remarkable linear relation with yield stress. As the twinning strain is higher than that of nominal yield strain of 0.2% [26]. It thus the twinning strengthen mechanism is not considered in the present study, and 1 wt.% C addition brings 180.71 MPa increment of yield stress in high manganese steel.

According to the above calculation, the contributions of Mn, Cr, Al, and C elements to yield stress are calculated to be 0, 39, 42, and 112 MPa, respectively. In total, solutes improvement of 193 MPa on yield stress illustrated in Table 2.

Precipitation Strengthening

As discussed above, the effect of calculated contribution of grain boundary, solutes, and precipitation to yield stress are concluded in Table 2. Due to the overall yield strength comes from the three factors, including grain boundary, solutes, and carbide precipitation. Therefore, the value of strengthening contribution of carbides precipitation is the gap between overall yield strength and the sum of grain boundary and solutes strengthening contributions.

The result shows that the precipitation ($Fe(Mn)_3C$ carbide) contributes more than 100 MPa to yield stress after individual 1100 °C solution treatment, as well as combined 1100 °C solution + 300 °C aging treatment. However, with increasing the aging temperature, the precipitation located along the grain boundary and inside the grain dissolved into matrix microstructure as compared and discussed above. In the meanwhile, the yield stress contribution from precipitation decreases to 45 MPa only. The present calculation result corresponds well with the microstructure evolution and previous similar studies [29], especially providing a clear relation between the yield stress and carbide precipitation.

Kang et al. [20] point out that precipitation phase ($Fe(Mn)_3C$ carbide) starts at the temperature of 800 °C, indicating the $Fe(Mn)_3C$ carbide forming during the solution treatment. Meanwhile, Mueller et al. [30] predict that the carbide start to dissolve in ferrite at 650 °C, as well as that the dissolution of carbide is rapid in austenite [31]. Therefore, the $Fe(Mn)_3C$ carbide shall dissolve into the austenite microstructure during the aging treatment with above 400 °C temperature, as illustrated in Fig. 2c and d. Zheng and Li [32] propose the direct evidence that the submicron-scale carbide particles enhances the density of geometrically necessary dislocations at the strain of 0.6% (close to the yield strain point) resulting in higher yield stress and work-hardening rate. In the meanwhile, the present observation (Fig. 3c) supports that the nanoscale carbides pin the sliding dislocation, bringing considerable strength improvement. Thus, the 1100 °C solution treated ZG4Al steel with lower than 300 °C aging treatment has higher yield stress. With further aging temperature increasing, the yield stress decreases accompanying with precipitation dissolution. The similar over aging of precipitates also plays an important role in weakening the yield strength of Inconel 718 alloy [33]. Furthermore, excluding aging treatment, the radiation-induced Ostwald ripening also determines the precipitates overgrowing [34].

Conclusion

In summary, with the design of the solution and aging treatments, the morphology and distribution of the $Fe(Mn)_3C$ carbide can be controlled. Subsequently, the mechanical properties, especially the yield strength of the Fe-18.4Mn-2.1Cr-1.3C-4Al (wt.%) steel is adjusted under certain heat treatment condition. In detail, the contribution of $Fe(Mn)_3C$ carbide, grain boundary, as well as solutes to yield stress are systematically investigated as:

(1) With the 1100 °C solution and 300 °C aging treatment, the $Fe(Mn)_3C$ carbides are commonly observed along the grain boundary and inside the grain. While the carbides gradually dissolve with increasing aging temperature up to 500 °C;
(2) The contribution of the carbides to yield stress achieves above 100 MPa after 1100 °C solution with or without 300 °C aging treatment. With the aging temperature increasing to 500 °C, the carbides play a minor effect on yield stress improvement.

Acknowledgments This work was supported by Guangdong Province Key Area R&D Program (Grant no. 2020B0101340004), International Science and Technology Cooperation Project of Guangdong Province (Grant no. 2021A0505030051), Innovation and Technology Fund (ITF) (Grant no. ITP/021/19AP) and Science and Technology Planning Project of Guangzhou (Grant no. 201907010026).

Declarations

Conflict of interest On behalf of all authors, the corresponding author states that there is no conflict of interest.

References

1. L. Li, The status and approach of energy-saving and emission reduction in iron & steel industry. Mater. Res. Appl. **2**(4), 328–331 (2008)
2. S.S. Sohn, K. Choi, J.-H. Kwak, N.J. Kim, S. Lee, Novel ferrite–austenite duplex lightweight steel with 77% ductility by transformation induced plasticity and twinning induced plasticity mechanisms. Acta Mater. **78**, 181–189 (2014)
3. J.H. Hwang, T.T.T. Trang, O. Lee, G. Park, A. Zargaran, N.J. Kim, Improvement of strength – ductility balance of B2-strengthened lightweight steel. Acta Mater. **191**, 1–12 (2020)
4. S. Kim, S. Ohtsuka, T. Kaito, S. Yamashita, M. Inoue, T. Asayama, T. Shobu, Formation of nano-size oxide particles and δ-ferrite at elevated temperature in 9Cr-ODS steel. J. Nucl. Mater. **417**(1), 209–212 (2011)
5. V.A. Hosseini, K. Hurtig, D. Gonzalez, J. Oliver, N. Folkeson, M. Thuvander, K. Lindgren, L. Karlsson, Precipitation kinetics of Cu-rich particles in super duplex stainless steels. J. Market. Res. **15**, 3951–3964 (2021)
6. G. Frommeyer, U. Brüx, Microstructures and mechanical properties of high-strength Fe–Mn–Al–C light-weight TRIPLEX steels. Steel Res. Int. **77**(9–10), 627–633 (2006)
7. M. Ferrante, M. De Mello, A. Lesko, SAF 2205 duplex stainless steel HAZ microstructural changes during long term ageing at 380 C. KOVOVE MATERIALY. **37**, 120–128 (1999)
8. Fu. Peng, Z.-b Zheng, W.-p Yang, H.-k Yang, Influence of carbon addition on mechanical properties of Fe–Mn–C twinning-induced plasticity steels. J. Iron Steel Res. Int. **29**(9), 1446–1454 (2021). https://doi.org/10.1007/s42243-021-00688-x
9. J. Bystrzycki, A. Fraczkiewicz, R. Łyszkowski, M. Mondon, Z. Pakieła, Microstructure and tensile behavior of Fe–16Al-based alloy after severe plastic deformation. Intermetallics. **18**(7), 1338–1343 (2010)
10. H. Ban, G. Shi, Y. Shi, Y. Wang, Overall buckling behavior of 460MPa high strength steel columns: experimental investigation and design method. J. Constr. Steel Res. **74**, 140–150 (2012)
11. E. Ma, T. Zhu, Towards strength–ductility synergy through the design of heterogeneous nanostructures in metals. Mater. Today. **20**(6), 323–331 (2017)
12. C. Haase, C. Zehnder, T. Ingendahl, A. Bikar, F. Tang, B. Hallstedt, W. Hu, W. Bleck, D.A. Molodov, On the deformation behavior of κ-carbide-free and κ-carbide-containing high-Mn lightweight steel. Acta Mater. **122**, 332–343 (2017)
13. W.J. Lu, X.F. Zhang, R.S. Qin, κ-carbide hardening in a low-density high-Al high-Mn multiphase steel. Mater. Lett. **138**, 96–99 (2015)
14. B.B. Lindahl, M. Selleby, The Al–Fe–Mn system revisited—An updated thermodynamic description using the most recent binaries. Calphad. **43**, 86–93 (2013)
15. K. Ishida, H. Ohtani, N. Satoh, R. Kainuma, T. Nishizawa, Phase equilibria in Fe–Mn–Al–C alloys. ISIJ Int. **30**(8), 680–686 (1990)
16. J.-E. Jin, Y.-K. Lee, Microstructure and mechanical properties of Al-added high Mn austenitic steel, in *Advanced steels*. ed. by

Y. Weng, H. Dong, Y. Gan (Springer Berlin Heidelberg, Berlin, Heidelberg, 2011), pp. 259–264 https://doi.org/10.1007/978-3-642-17665-4_26
17. T. Shun, C.M. Wan, J.G. Byrne, A study of work hardening in austenitic Fe–Mn–C and Fe–Mn–Al–C alloys. Acta Metall. Mater. **40**(12), 3407–3412 (1992)
18. B. Mehta, K. Frisk, L. Nyborg, Effect of precipitation kinetics on microstructure and properties of novel Al–Mn–Cr–Zr based alloys developed for powder bed fusion – laser beam process. J. Alloy. Compd. **920**, 165870 (2022)
19. F. Nurjaman, F. Bahfie, W. Astuti, A. Shofi, The effect of solid solution treatment on the hardness and microstructure of 0.6% wt C-10.8% wt. Mn-1.44% wt. Cr austenitic manganese steel. J. Phys. Conf. Ser. **817**, 012066 (2017)
20. S. Kang, Y.-S. Jung, J.-H. Jun, Y.-K. Lee, Effects of recrystallization annealing temperature on carbide precipitation, microstructure, and mechanical properties in Fe-18Mn-0.6C-1.5Al TWIP steel. Mater. Sci. Eng. A. **527**(3), 745–751 (2010)
21. H. Shufen, Z. Zhibin, Y. Weiping, Y. Haokun, Fe–Mn–C–Al low density steel for structural materials: a review of alloying, treatment, microstructure and mechanical properties. Steel Res. Int. **93**(9), 2200191 (2022). https://doi.org/10.1002/srin.202200191
22. S. Chen, R. Rana, A. Haldar, R.K. Ray, Current state of Fe-Mn–Al–C low density steels. Prog. Mater Sci. **89**, 345–391 (2017)
23. Y.Z. Tian, Y. Bai, M.C. Chen, A. Shibata, D. Terada, N. Tsuji, Enhanced strength and ductility in an ultrafine-grained Fe-22Mn-0.6C austenitic steel having fully recrystallized structure. Metall Mater Trans A. **45**(12), 5300–5304 (2014)
24. S.X. Ding, C.P. Chang, J.F. Tu, K.C. Yang, Microstructure and tensile behaviour of 15–24 wt.-%Mn TWIP steels. Mater. Sci. Technol. **29**(9), 1048–1054 (2013)
25. X. Yuan, Y. Zhao, X. Li, L. Chen, Effect of Cr on mechanical properties and corrosion behaviors of Fe–Mn–C–Al–Cr–N TWIP steels. J. Mater. Sci. Technol. **33**(12), 1555–1560 (2017)
26. H.K. Yang, Y.Z. Tian, Z.F. Zhang, Revealing the mechanical properties and microstructure evolutions of Fe–22Mn–0.6C–(x) Al TWIP steels via Al alloying control. Mater. Sci. Eng. A. **731**, 61–70 (2018)
27. H.K. Yang, V. Doquet, Z.F. Zhang, Micro-scale measurements of plastic strain field, and local contributions of slip and twinning in TWIP steels during in situ tensile tests. Mater. Sci. Eng. A. **672**, 7–14 (2016)
28. C.W. Shao, P. Zhang, R. Liu, Z.J. Zhang, J.C. Pang, Z.F. Zhang, Low-cycle and extremely-low-cycle fatigue behaviors of high-Mn austenitic TRIP/TWIP alloys: property evaluation, damage mechanisms and life prediction. Acta Mater. **103**, 781–795 (2016)
29. G. Yang, J.-K. Kim, An overview of high yield strength twinning-induced plasticity steels. Metals. **11**(1), 124 (2021)
30. J.J. Mueller, X. Hu, X. Sun, Y. Ren, K. Choi, E. Barker, J.G. Speer, D.K. Matlock, E. De Moor, Austenite formation and cementite dissolution during intercritical annealing of a medium-manganese steel from a martensitic condition. Mater. Des. **203**, 109598 (2021)
31. G. Molinder, A quantitative study of the formation of austenite and the solution of cementite at different austenitizing temperatures for a 1.27% carbon steel. Acta Metall. **4**(6), 565–571 (1956)
32. C. Zheng, L. Li, Mechanical behavior of ultrafine-grained eutectoid steel containing nano-cementite particles. Mater. Sci. Eng. A. **713**, 35–42 (2018)
33. D. Sindhura, M.V. Sravya, G.V.S. Murthy, Comprehensive microstructural evaluation of precipitation in inconel 718. Metallogr. Microstruct. Anal. **8**(2), 233–240 (2019)
34. M.L. Lescoat, J. Ribis, Y. Chen, E.A. Marquis, E. Bordas, P. Trocellier, Y. Serruys, A. Gentils, O. Kaïtasov, Y. de Carlan, A. Legris, Radiation-induced Ostwald ripening in oxide dispersion strengthened ferritic steels irradiated at high ion dose. Acta Mater. **78**, 328–340 (2014)